



A new labdane-type diterpenoid from leaves of *Vitex rotundifolia*

Yusuke Hanaki^{*}, Rintaro Abe, Yasunori Sugiyama, Yasumasa Hara, Ryo C. Yanagita

Department of Applied Biological Science, Faculty of Agriculture, Kagawa University, 2393, Ikenobe, Miki, Kita, Kagawa 761-0795, Japan

ARTICLE INFO

Keywords:

Labdane-Type Diterpenoid
Vitex rotundifolia
 Cytotoxicity

ABSTRACT

Vitex rotundifolia is a folk medicinal plant that has been used to treat various diseases. We have previously found that the extract of its leaves shows cytotoxic and epithelial mesenchymal transition inhibitory effect in HHUA endometrial cells. In this study, a new labdane-type diterpenoid **1** was isolated and its structure was elucidated by NMR and CD spectroscopic analysis followed by density functional theory calculations. Compound **1** showed cytotoxicity toward HHUA cells with an IC₅₀ value of 6.4 μM, but did not inhibit phorbol ester-induced epithelial mesenchymal transition nor lipopolysaccharide-stimulated nitric oxide production.

1. Introduction

Vitex is a genus in the Lamiaceae family, consisting of more than 200 species. Some *Vitex* plants have been used as traditional medicine for the treatment of various diseases [1,2]. *Vitex rotundifolia* is widely distributed on the Asian and Oceanian coasts, and its fruits (“Mankeishi” in Japanese) have been used as a herbal medication for the treatment of colds, headaches, and other inflammatory symptoms [1]. The fruit of *V. agnus-castus* (chasteberry) is a folk treatment for premenstrual syndrome, menstrual pain, and menopausal symptoms. In addition, the extract of its fruit was reported to inhibit growth activity in cancer cells *in vitro* and *in vivo* [3]. Various terpenoids contained in these plants have drawn attention due to their anti-inflammatory, anti-tumor, anti-bacterial, and other pharmacological activities [4]. We have recently found that the leaf extract of *V. rotundifolia* showed an epithelial-mesenchymal transition (EMT) inhibitory effect in HHUA endometrial cancer cells, and vitetrolin D, a halimane-type diterpenoid, was isolated as the active compound [5]. Since endometrial EMT is a plausible factor promoting endometriosis, adenomyosis, and endometrial cancer [6,7], these findings could provide an explanation for why *Vitex* fruits have been used in the treatment of gynecological disorders. Additionally, we have also observed that the extract of *V. rotundifolia* exhibited cytotoxicity against HHUA cells, suggesting the presence of other anti-cancer candidates in this plant. In our continuing study on cytotoxic and anti-proliferative natural products in *V. rotundifolia*, we, in this study, isolated an undescribed labdane-type diterpenoid **1** with cytotoxicity against the HHUA cell line.

2. Results and discussion

2.1. Isolation and structural determination of **1**

The fresh leaves (4.6 kg) were extracted with MeOH, and partitioned between *n*-hexane and 90 % MeOH in H₂O. The *n*-hexane layer was subjected to silica gel column chromatography, ODS column chromatography, and reversed-phase HPLC to give **1** (2.7 mg) as a 3:1 inseparable mixture of two diastereomers (**1a/1b**, Fig. 1A). Compound **1** was obtained as a colorless syrup with an optical rotation of $[\alpha]_D^{24} = -15.4$ (c 0.1, MeOH). The molecular formula of **1** was determined to be C₂₂H₃₆O₅ by HR-ESI-MS *m/z* 403.2469 (calcd for C₂₂H₃₆O₅Na, 403.2455). The IR spectrum suggested the presence of hydroxy and ester groups (3414, 1733 cm⁻¹). The ¹³C NMR and DEPT spectra showed duplicate resonances for three tertiary methyl groups (δ 19.9/19.8, 23.7/23.8, and 33.2/33.1), one secondary methyl group (δ 17.6/17.2), one oxygenated methylene (δ 77.7/78.4), seven methylenes (δ 18.8/18.8, 29.6/29.7, 33.6/34.0, 34.6/34.8, 36.4/36.6, 44.2/44.1, and 45.0/47.9), two oxygenated methines (δ 70.3/70.7 and 99.8/99.4), two methines (δ 31.6/31.4 and 49.8/48.7), two oxygenated quaternary carbons (δ 90.2/89.7 and 94.5/92.3), two quaternary carbons (δ 34.2/34.1 and 42.9/42.9), and an acetoxy group (δ 21.9/22.0 and 170.4/170.5). The planar structure of **1** was determined by COSY, HMQC, and HMBC experiments (Fig. 1B). The labdane structure (A and B rings) was confirmed by the HMBC correlations from H-1a to C2; H-5 to C19/C20; H-6 to C10; H₃-17 to C7/C8/C9; H₃-18 to C3/C4/C5/C19; H₃-19 to C3/C5/C18; and H₃-20 to C1/C5/C9/C10. The correlation from oxygenated methine H-6 to the carbonyl carbon suggested the presence of an acetoxy group at position

^{*} Corresponding author at: Faculty of Agriculture, Kagawa University, Ikenobe, Miki-cho, Kita, Kagawa 761-0795, Japan.

E-mail address: hanaki.yusuke@kagawa-u.ac.jp (Y. Hanaki).

6. The bis-spiro tetrahydrofuran structure (C and D rings) was confirmed by the HMBC correlation from H-8 to C11; H-14a to C13/C16; H-16b to C12/C15; H-16a to C13/C14; H₃-17 to C9; and H₃-20 to C9.

The NOESY cross-peaks suggested that the 6-acetoxy group, H-8, and H₃-20 exist at the same β -face of the AB ring. The relative configuration at C-9 and C-13 was established by the cross-peaks between H-11b and H₃-20, and H-16a and H₃-17, respectively (Fig. 1C). The ¹H NMR chemical shifts at H-15, H-16a, and H-16b were significantly different between **1a** and **1b**, while other signals were similar or overlapped each other. By comparison of ¹H NMR data of other labdane-type diterpenoids with the same spiro lactol ring [8–14], **1** was suggested to be a 3:1 diastereomeric mixture at position 15. We next performed molecular modeling to demonstrate the three-dimensional structure of both epimers at position 15. Their most stable conformations were predicted by the simulated annealing method and density functional theory (DFT) calculation (Fig. 2). The conformation of the epimer with an α -orientation of 15-OH showed an intramolecular hydrogen bond between 15-OH and oxygen atom in C-ring, while the epimer with a β -orientation of 15-OH did not form any intramolecular hydrogen bonds. The ¹H NMR coupling constant between H-15 and 15-OH ($J = 10.6$ Hz) in the major isomer **1a** suggested that the 15-OH group was involved in intramolecular hydrogen bond. In addition, the ¹H NMR chemical shifts at H-15, H-16a, and H-16b of **1a/1b** were well correlated to those of velutine A/15-*epi* velutine A [8], 15-*epi*-leoheteronone B/leoheteronone B,⁹ and 15-*epi*-lagopsin D/lagopsin D [10], which are the pairs of derivatives with α -/ β -orientation of 15-OH. Therefore, we concluded that the 15-OH group had an α -orientation in the major isomer **1a**, and a β -orientation in the minor isomer **1b**.

The absolute configuration of **1** was estimated to be the same as other related labdane-type diterpenoids occurring in Lamiaceae plants [15]. To reinforce the estimated absolute configuration assignment, we employed CD spectroscopic analysis. As shown in Fig. 3, the observed CD for **1** exhibited a Cotton effect at 213 nm ($\Delta\epsilon +1.1$). On the other hand, the calculated CD curve of (5S, 6R, 8R, 9R, 10S, 13R, 15R)-**1a** and (5S, 6R, 8R, 9R, 10S, 13R, 15S)-**1b** was obtained by the time-dependent density functional theory (TD-DFT) calculation. Because the calculated CD curve was consistent with the experimental spectrum, the absolute configurations of **1a** and **1b** were determined to be (5S, 6R, 8R, 9R, 10S, 13R, 15R) and (5S, 6R, 8R, 9R, 10S, 13R, 15S), respectively.

2.2. Cytotoxicity and EMT inhibitory activity of **1** in HHUA cells

First, we evaluated the cytotoxicity of **1** toward HHUA cells. After 24 h treatment with **1**, cell viability was determined by WST-based colorimetric assay (Fig. 4), and the IC₅₀ value (and the 95 % confidence interval) of **1** was found to be 6.4 μ M (4.5–9.0 μ M). Since *V. rotundifolia* has EMT inhibitory potential [5], we next tested the inhibitory activity of **1** against EMT in HHUA cells. Our previous study showed that 12-*O*-tetradecanoylphorbol 13-acetate (TPA) reduced the expression of E-cadherin, a main component of the epithelial adherens junction, and increased vimentin, an intermediate filament of mesenchymal cells [16]. Thus, it was evaluated by western blotting whether **1** suppressed the TPA-induced change in expression of these EMT marker proteins. Since

1 significantly decreased the cell viability at a concentration higher than 10 μ M (Fig. 4), we used 5 μ M of **1** in this assay. As shown in Fig. 5, **1** did not reduce the vimentin/E-cadherin ratio, suggesting that **1** was not an EMT inhibitor, at least at the non-toxic concentration.

2.3. Inhibitory activity of **1** against nitric oxide production in RAW264 cells

As mentioned above, some terpenoids isolated from *Vitex* plants showed the anti-inflammatory activity [4]. Therefore, we also evaluated the inhibitory effect of **1** on the production of nitric oxide (NO), an inflammatory mediator, in lipopolysaccharide (LPS)-stimulated RAW264 cells. The Griess assay [17] revealed that **1** failed to suppress the NO production at 10 μ M or below (Fig. 6), suggesting that **1** did not have anti-inflammatory properties.

2.4. Conclusions

In this study, we described the isolation of **1** from the leaves of *V. rotundifolia* and structural elucidation by NMR and CD spectroscopic analysis. These results revealed that **1** was an undescribed spiro labdane-type diterpenoid though some related derivatives have been previously reported [8–10,15,18]. Compound **1** did not inhibit EMT nor NO production, but was cytotoxic to the HHUA endometrial cancer cell line. Given the limited information on the biological activities of spiro labdane-type diterpenoids, our results provided some insights into their structure–activity relationship. Referring to previous reports, the cytotoxicity of **1** to cancer cells seems to be relatively stronger than those of other spiro labdane-type derivatives. Previtexilactone, whose D ring is 15,16- γ -lactone, did not show significant cytotoxicity against the HCT116 colon cancer cell line (IC₅₀ > 100 μ M) [19]. The cytotoxicity of nishindanol, which has the 13-*epi* configuration and 16,15- γ -lactol, was approximately one order of magnitude weaker than that of **1** (IC₅₀ for PANC1 and DU145 cell lines was 41 μ M and > 60 μ M, respectively) [20]. On the other hand, **1** did not inhibit the NO production, while negundoin E, which has the 13-*epi* configuration, 16,15- γ -lactol, and an acetoxy group at position 3 instead of position 6, was reported to show a strong inhibitory activity (IC₅₀ = 0.23 μ M) [21]. Therefore, the structure of D-ring and the substitution position of the acetoxy group on the AB-rings should have significant effects on their cytotoxicity and anti-inflammatory activity. We have started the synthetic study of these derivatives to simultaneously evaluate their biological activity under the same assay conditions.

3. Materials and methods

3.1. General remarks

NMR spectra were recorded on JNM-ECZ500 (JEOL, Tokyo, Japan), and chemical shifts are reported in ppm relative to the residual solvent (¹H NMR: CDCl₃ as $\delta = 7.26$ ppm, ¹³C NMR: CDCl₃ as $\delta = 77.0$ ppm). High-resolution electrospray ionization mass spectra (HR-ESI-qTOF-MS) were recorded on a micrOTOF II (Bruker Daltonics, Billerica, MA,

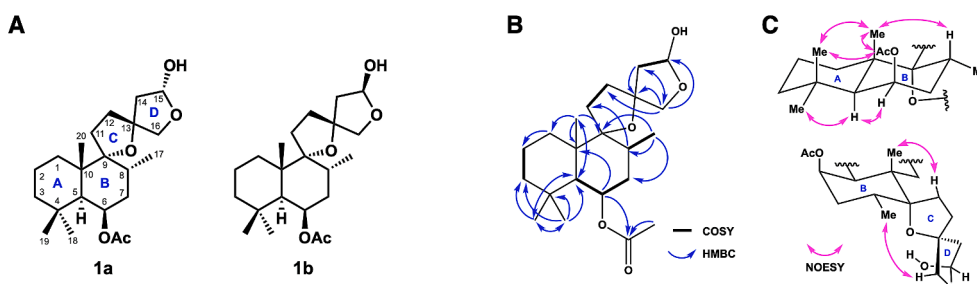


Fig. 1. (A) Structure of **1a** and **1b**. (B) COSY and HMBC correlations of **1**. (C) Key NOESY correlations of **1a**.

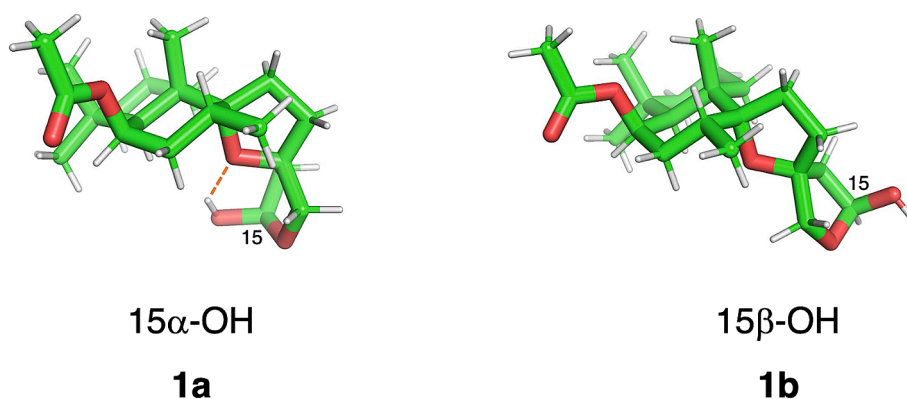


Fig. 2. The most stable conformations of epimers at position 15 of **1**.

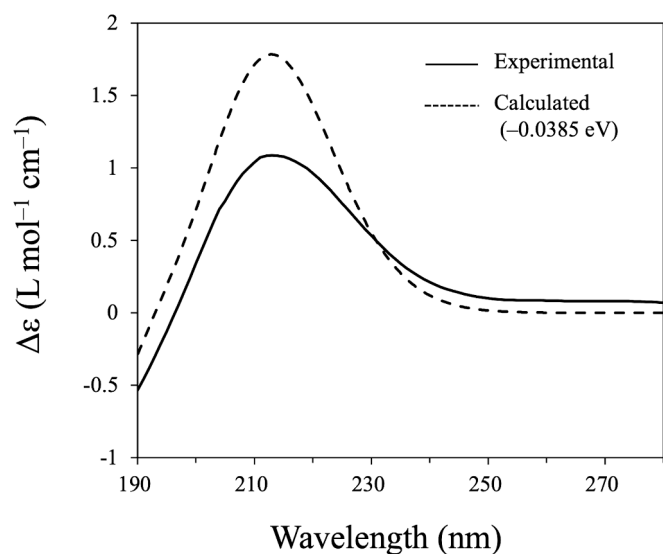


Fig. 3. Experimental and calculated CD spectra of **1**.

USA). Optical rotations were measured with a P-1010 digital polarimeter (JASCO, Tokyo, Japan). Infrared (IR) spectra were recorded on a FT/IR-670 Plus (JASCO) and are reported in wave numbers (cm^{-1}). CD spectra were recorded on a J-1100 spectropolarimeter (JASCO). Wakogel C-300 (FUJIFILM Wako Pure Chemical Corporation, Osaka, Japan) and COSMOSIL 75C18-OPN (Nacalai tesque, Inc., Kyoto, Japan) were used for column chromatography. YMC Pack ODS-AM AM12S05-1520 wt (YMC Co. Ltd., Kyoto, Japan) was used for HPLC.

3.2. Extraction and isolation

The plant *Vitex rotundifolia* L. f. (Lamiaceae) was collected from Chidorigahama Beach (Naruto, Japan) in November 2022. The voucher specimen was deposited at the Department of Applied biological Science, Kagawa University. Fresh leaves of *V. rotundifolia* (4.6 kg) were extracted with methanol (10 L) at room temperature. The methanol extract (350 g) was partitioned between *n*-hexane and 90 % methanol in H_2O . The *n*-hexane extract (11.6 g) was subjected to silica gel column chromatography (ϕ 40 x 460 mm; 0–100 % EtOAc in *n*-hexane) to give 7 fractions. The elute obtained with 40 % EtOAc in *n*-hexane (0.75 g) was subjected to ODS column chromatography (ϕ 25 x 100 mm; 50–100 % MeOH in H_2O , and EtOH) to give 6 fractions. The elute obtained with 80 % MeOH in H_2O (104 mg) was further purified by HPLC. The elute (30 mg) was subjected to reversed-phase HPLC (YMC Pack ODS-AM AM12S05-1520 wt, ϕ 20 x 150 mm; 80 % MeOH in H_2O ; flow rate 8.0 mL/min, retention time 15.1–16.5 min) to give **1** (2.7 mg) as a

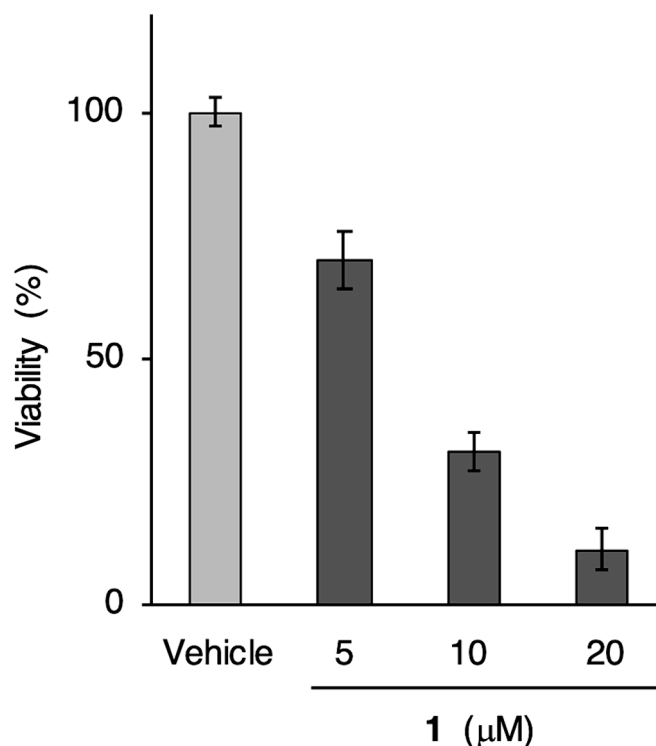


Fig. 4. Effects of **1** on the cell viability of HHUA cells. HHUA cells were treated with the indicated concentration of **1** for 24 h. Thereafter, cell viability was determined by WST assay. Cell growth was expressed as a percentage relative to the vehicle group. Error bars represent standard error ($n = 4$). A result of one of the three independent experiments that gave similar results is shown.

colorless syrup; $[\alpha]_{\text{D}}^{24} = -15.4$ (c 0.1, MeOH); CD (0.00026 M, MeOH) $\lambda_{\text{max}} (\Delta\epsilon)$ 213 (+1.1) nm; IR (KBr; cm^{-1}): 3414, 2925, 1733, 1250, 1223, 1021; HR-ESI-qTOF-MS: m/z 403.2469 $[\text{M} + \text{Na}]^+$ (calcd for $\text{C}_{22}\text{H}_{36}\text{O}_5\text{Na}$, 403.2455); ^1H and ^{13}C NMR spectra data: see Table 1.

3.3. Molecular modeling and CD calculation

The conformer library of **1a** and **1b** was generated by a simulated annealing method under a vacuum using the GROMACS program (version 2023.3) with a general AMBER force field 2 (GAFF2) and the AM1-BCC charge. Then, two possible conformers from each compound were selected, which were within 3 kcal/mol from the global minimum conformer for each compound at the B3LYP/6-31G(d) level of theory. Further structural optimization and frequency analysis were performed at the M06-2X/jul-cc-pVTZ level of theory with polarizable continuum

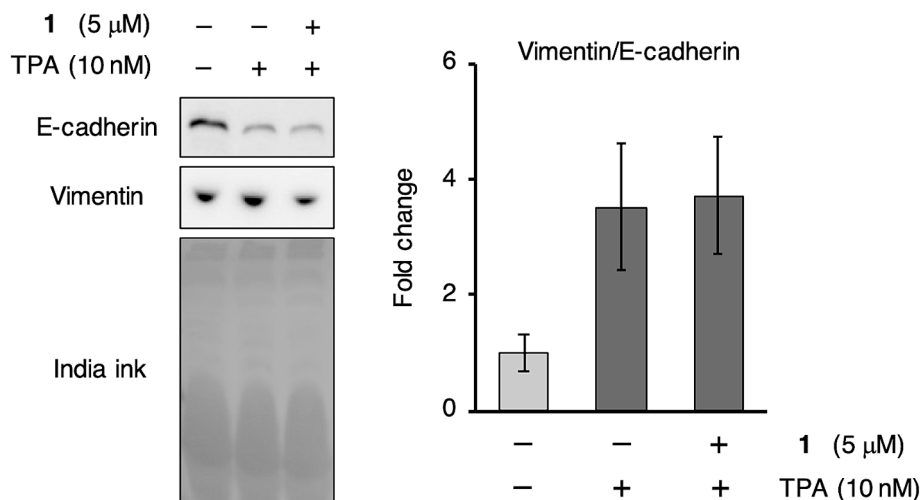


Fig. 5. Effect of **1** on the expressions of EMT marker proteins in TPA-stimulated HHUA cells. A representative result of western blotting and quantification of band intensity from triplicate samples are shown. Error bars represent standard error ($n = 3$).

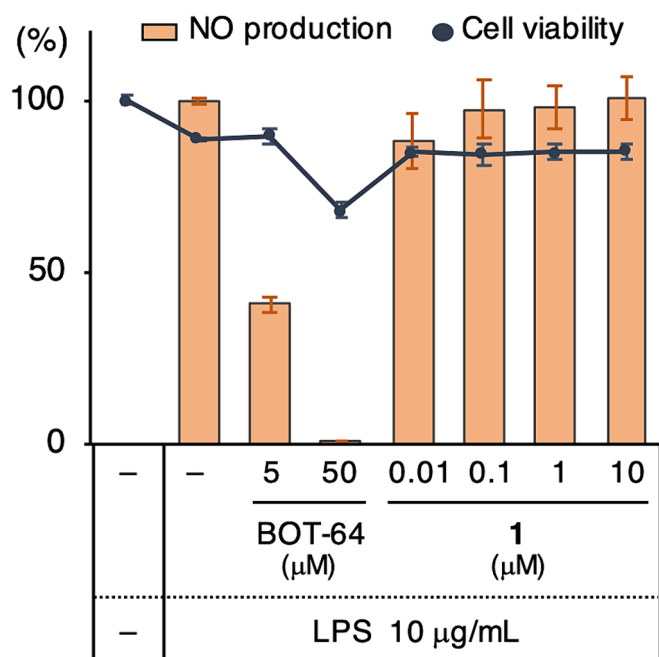


Fig. 6. Effect of **1** on the NO production in LPS-stimulated RAW264 cells. BOT-64 (NF- κ B inhibitor) was used as a positive control. A representative result of two independent experiments that gave similar results is shown. Error bars represent standard error ($n = 3$).

model using the integral equation formalism (IEFPCM) solvent model with methanol solvent. The optimized structures were subjected to the time-dependent density functional theory (TD-DFT) calculation at the M06-2X/jul-cc-pVTZ level of theory with the IEFPCM solvent (methanol) model. The four calculated ECD spectra were combined with the weight based on the DFT free energy difference and slightly shifted to fit the experimental spectra. All DFT calculations were performed using the Gaussian 16 (Revision C.02) program.

3.4. Cell culture

HHUA (RCB0658) human endometrial cancer and RAW264 (RCB0535) mouse macrophage cell lines were provided by RIKEN BRC through National Bio-Resource Project of the NEXT/AMED (Tsukuba,

Table 1
NMR data of **1** in CDCl₃.

position	1a/1b	
	δ_H (J, Hz)	δ_C
1a	1.54 (1H, m)	34.6 / 34.8
1b	1.47 (1H, m)	
2a	1.66 (1H, m)	18.8 / 18.8
2b	1.54 (1H, m)	
3a	1.33 (1H, m)	44.2 / 44.1
3b	1.11 (1H, m)	
4		34.2 / 34.1
5	1.30 (1H, m)	49.8 / 48.7
6	5.38 (1H, m)	70.3 / 70.7
7a	1.72 (1H, m)	36.4 / 36.6
7b	1.50 (1H, m)	
8	2.12 (1H, m)	31.6 / 31.4
9		94.5 / 92.3
10		42.9 / 42.9
11a	2.18 (1H, m)	29.6 / 29.7
11b	1.73 (1H, m)	
12a	2.16 (1H, m)	33.6 / 34.0
12b	1.89 (1H, m)	
13		90.2 / 89.7
14a	2.46 (1H, d, 13.2) / 2.40 (1H, dd, 13.2, 5.2)	45.0 / 47.9
14b	1.85 (1H, dd, 13.2, 5.2) / 1.93 (1H, m)	
15	5.41 (1H, dd, 10.6, 4.8) / 5.61 (1H, br d, 5.1)	99.8 / 99.4
16a	4.25 (1H, d, 8.7) / 4.02 (1H, d, 8.6)	77.7 / 78.4
16b	3.72 (1H, d, 8.7) / 3.96 (1H, d, 8.6)	
17	0.84 (3H, d, 6.9) / 0.79 (3H, d, 6.3)	17.6 / 17.2
18	0.92 (3H, s)	33.2 / 33.1
19	0.98 (3H, s)	23.7 / 23.8
20	1.24 (3H, s)	19.9 / 19.8
C=O		170.4 / 170.5
COCH ₃	2.04 (3H, s)	21.9 / 22.0
15-OH	3.96 (1H, br d, 10.9)	

Japan). HHUA cells were cultured in Ham's/F² medium with 10 % heat-inactivated FBS, 1 mM L-glutamine, 100 U/mL penicillin, and 100 μg/mL streptomycin. RAW264 cells were cultured in DMEM medium with 10 % heat-inactivated FBS, 1 mM L-glutamine, 100 U/mL penicillin, and 100 μg/mL streptomycin. They were maintained at 37 °C in a humidified atmosphere containing 5 % CO₂.

3.5. Cytotoxicity assay

HHUA cells (1 x 10⁴ cells/200 μL/well) were seeded in 96-well plate and allowed to attach overnight. Thereafter, solution of **1** in DMSO or DMSO alone was added. After incubation for 24 h, 20 μL of Cell Counting

Kit-8 (FUJIFILM Wako Pure Chemical Corporation, Osaka, Japan) was added to each well, and plate was incubated at 37 °C for an additional 4 h. The absorbance at 450 nm was measured for the control (C) well and the test well (T) using a microplate reader (Multiskan FC; Thermo Fisher Scientific, Waltham, MA, USA). Cell viability in the presence of each concentration (5, 10, 20 μM) of **1** was calculated as $100 \times (T/C)$ using average of quadruplicate points. IC₅₀ value, defined as $100 \times (T/C) = 50$, was determined by processing these values.

3.6. Western blotting

0.2 % of atelocollagen solution (KOKEN Co., Ltd, Tokyo, Japan) was added to each well of a 48-well plate (150 μL/well) and incubated at 37 °C for 2 h to allow gelation. HHUA cells (7.5×10^4 cells/450 μL-well) were seeded in a collagen gel-coated 48-well plate and allowed to attach overnight, and then solution of **1** in DMSO or DMSO alone was added. After incubation for 30 min, TPA solution in DMSO or DMSO alone was added and incubated for 24 h. Cells and collagen gels were washed with PBS, lysed by adding 100 μL of 2X SDS sample buffer, and boiled for 10 min. Equal amounts of sample were subjected to SDS-PAGE using slab gels consisting of a 10 % acrylamide separation gel and a 3 % stacking gel, and transferred to a nitrocellulose membrane. After blocking with PBS-T containing 0.5 % skimmed milk for 1 h at room temperature, the blots were incubated for 2 h at room temperature with primary antibodies. After washing with PBS-T, the blots were incubated for 1 h at room temperature with secondary antibodies. After washing, the chemiluminescence signal of each band was quantified using Amersham Imager 680 analysis software (GE healthcare, Chicago, IL, USA). Anti-E-cadherin (24E10), anti-vimentin (D21H3), and HRP-conjugated anti-rabbit IgG antibodies were obtained from Cell Signaling Technology (Danvers, MA, USA). These antibodies were diluted 1:1000 and used for the detection of immunoreactive bands. Total proteins were stained with India ink as loading control.

3.7. Measurement of NO production

RAW264 cells (1×10^4 cells/200 μL-well) were seeded in a black 96-well plate and allowed to attach overnight. The supernatant was aspirated and 180 μL of fresh medium containing each test compound was added. After incubation for 2 h, 20 μL of fresh medium containing lipopolysaccharide (LPS) was added (10 μg/mL, final concentration) and incubated for 24 h. Aliquots of supernatant (50 μL) were incubated with 50 μL of Griess reagent (1 % sulfanilamide and 0.1 % naphthylethylenediamine in 2.5 % phosphoric acid), and the absorbance at 570 nm was measured using a microplate reader (Multiskan FC). The remaining supernatant was aspirated from the black 96-well plate, and 100 μL of phosphate buffered saline containing 10 μg/mL of fluorescein diacetate was added. After incubation for 1 h, the fluorescence intensity (excitation and emission at 485 nm and 538 nm, respectively) was measured using Fluoroskan Ascent (Thermo Fisher Scientific).

CRedit authorship contribution statement

Yusuke Hanaki: Writing – original draft, Validation, Investigation, Data curation, Conceptualization. **Rintaro Abe:** Investigation, Data curation. **Yasunori Sugiyama:** Writing – review & editing, Validation, Investigation. **Yasumasa Hara:** Writing – review & editing, Validation, Investigation. **Ryo C. Yanagita:** Writing – review & editing, Validation, Investigation.

Declaration of competing interest

The authors declare that they have no known competing financial interests or personal relationships that could have appeared to influence the work reported in this paper.

Acknowledgements

The authors thank Ms. Tsugumi Shiokawa and Dr. Hiroko Tada (Okayama University) for MS measurement, and Mr. Takeru Fujita and Prof. Masahiro Ogawa (Kagawa University) for CD measurement. The DFT calculation was performed using Research Center for Computational Sciences, Okazaki, Japan. This research was supported by Kagawa University Research Promotion Program 2023 (Grant Number 23K0F013 and 23K0C003).

Appendix A. Supplementary data

Supplementary data to this article can be found online at <https://doi.org/10.1016/j.rechem.2024.101512>.

References

- [1] C.-X. Yan, Y.-W. Wei, H. Li, K. Xu, R.-X. Zhai, D.-C. Meng, X.-J. Fu, X. Ren, L. F. Vitex Rotundifolia, L. Vitex Trifolia, A review on their traditional medicine, phytochemistry, pharmacology, J. Ethnopharmacol. 308 (2023) 116273.
- [2] A. Rani, A. Sharma, The genus vitex: a review, Pharmacogn. Rev. 7 (14) (2013) 188–198.
- [3] M. Imai, B. Yuan, H. Kikuchi, M. Saito, K. Ohyama, C. Hirobe, T. Oshima, T. Hosoya, H. Morita, H. Toyoda, Growth Inhibition of a Human Colon Carcinoma Cell, COLO 201, by a Natural Product, Vitex Agnus-Castus Fruits Extract, *in Vivo* and *in Vivo*, Adv. Biol. Chem. 2 (1) (2012) 20–28.
- [4] J.-L. Yao, S.-M. Fang, R. Liu, M.B. Oppong, E.-W. Liu, G.-W. Fan, H. Zhang, A Review on the Terpenes from Genus Vitex, Molecules 21 (9) (2016) 1179.
- [5] Y. Hanaki, N. Iwase, Y. Sugiyama, S. Miyoshi, R.C. Yanagita, Cell Morphology-Based Screening Identified Vitetrolin D from Vitex Rotundifolia as an Inhibitor of Phorbol Ester-Induced Downregulation of E-Cadherin in HHUA Endometrial Cells, BPB Reports 6 (3) (2023) 103–107.
- [6] X. Liu, M. Shen, Q. Qi, H. Zhang, S.-W. Guo, Corroborating Evidence for Platelet-Induced Epithelial-Mesenchymal Transition and Fibroblast-to-Myofibroblast Transdifferentiation in the Development of Adenomyosis, Hum. Reprod. 31 (4) (2016) 734–749.
- [7] J. Bartley, A. Jülicher, B. Hotz, S. Mechsner, H. Hotz, Epithelial to Mesenchymal Transition (EMT) Seems to Be Regulated Differently in Endometriosis and the Endometrium, Arch. Gynecol. Obstet. 289 (4) (2014) 871–881.
- [8] A. Karioti, J. Heilmann, H. Skaltsa, Labdane Diterpenes from Marrubium Velutinum and Marrubium Cylleum, Phytochemistry 66 (9) (2005) 1060–1066.
- [9] P.M. Giang, P.T. Son, M. Katsuyoshi, H. Otsuka, New Bis-Spiroabdone-Type Diterpenoids from Leonurus Heterophyllus S, Chem. Pharm. Bull. 53 (11) (2005) 1475–1479.
- [10] H. Li, M.-M. Li, X.-Q. Su, J. Sun, Y.-F. Gu, K.-W. Zeng, Q. Zhang, Y.-F. Zhao, D. Ferreira, J.K. Zjawiony, J. Li, P.-F. Tu, Anti-Inflammatory Labdane Diterpenoids from Lagopsis Supina, J. Nat. Prod. 77 (4) (2014) 1047–1053.
- [11] D. Tasdemir, A.D. Wright, O. Sticher, I. Çalis, A. Linden, Detailed ¹H- and ¹³C-Nmr Investigations of Some Diterpenes Isolated from Leonurus Persicus, J. Nat. Prod. 58 (10) (1995) 1543–1554.
- [12] D. Tasdemir, A.D. Wright, O. Sticher, I. Çalis, New Furanoid and Seco-Labdanoic Diterpenes from Leonurus Persicus, J. Nat. Prod. 59 (2) (1996) 131–134.
- [13] D. Tasdemir, O. Sticher, I. Çalis, A. Linden, Further Labdane Diterpenoids Isolated from Leonurus Persicus, J. Nat. Prod. 60 (9) (1997) 874–879.
- [14] D. Tasdemir, I. Çalis, O. Sticher, Labdane Diterpenes From Leonurus Persicus, Phytochemistry 49 (1) (1998) 137–143.
- [15] H. Wu, J. Li, F.R. Fronczek, D. Ferreira, C.L. Burandt, V. Setola, B.L. Roth, J. K. Zjawiony, Labdane Diterpenoids from Leonotis Leonurus, Phytochemistry 91 (2013) 229–235.
- [16] Y. Hanaki, S. Miyoshi, Y. Sugiyama, R.C. Yanagita, M. Sato, 12-O-Tetradecanoylphorbol 13-Acetate Promotes Proliferation and Epithelial-Mesenchymal Transition in HHUA Cells Cultured on Collagen Type I Gel: A Feasible Model to Find New Therapies for Endometrial Diseases, Biosci. Biotechnol. Biochem. 86 (10) (2022) 1417–1422.
- [17] P. Griess, Bemerkungen Zu Der Abhandlung Der HH. Weselsky Und Benedikt "Ueber Einige Azoverbindungen", Ber. Dtsch. Chem. Ges. 12 (1) (1879) 426–428.
- [18] D. Rigano, A. Grassia, M. Bruno, S. Rosselli, F. Piozzi, C. Formisano, N.A. Arnold, F. Senatore, Labdane Diterpenoids from Marrubium Globosum Ssp. Libanoticum, J. Nat. Prod. 69 (5) (2006) 836–838.
- [19] P. Luo, Q. Yu, S.-N. Liu, W.-J. Xia, Y.-Y. Fang, L.-K. An, Q. Gu, J. Xu, Diterpenoids with Diverse Scaffolds from Vitex Trifolia as Potential Topoisomerase I Inhibitor, Fitorapia 120 (2017) 108–116.
- [20] M.A. Arai, T. Fujimatsu, K. Uchida, S.K. Sadhu, F. Ahmed, M. Ishibashi, Hh Signaling Inhibitors from Vitex Negundo; Naturally Occurring Inhibitors of the GLL1-DNA Complex, Mol. Biosyst. 9 (5) (2013) 1012–1018.
- [21] C.-J. Zheng, B.-K. Huang, Y. Wang, Q. Ye, T. Han, Q.-Y. Zhang, H. Zhang, L.-P. Qin, Anti-Inflammatory Diterpenes from the Seeds of Vitex Negundo, Bioorg. Med. Chem. 18 (1) (2010) 175–181.